Recent Tests of ALMA Circular Polarization Calibration and Imaging in Band 3

Crystal Brogan, Todd Hunter, & George Moellenbrock

September 30, 2015

Abstract

We present the observations, analysis, and results of experiments designed to assess the feasibility of observing and calibrating circularly polarized line emission with ALMA in Band 3. We describe the current polarization calibration path in CASA and provide useful recommendations for assessing the quality of the calibration. Attempts to observe circular polarization in an astronomical object were made initially in the CN 1-0 transition toward M17-SW, but primarily in the 95.1 GHz Class I CH_3OH maser toward G06.05. Although we do confirm the expected effect of the Stokes V leakage pattern, we cannot reproduce the residual Stokes V spectral line signal between different observing dates, nor between small offsets in the phase center observed within the same execution and session. This inconsistency precludes any attempt at measuring a believable magnetic field via the Zeeman effect at present. In contrast, the shapes of the calibrated Q and U spectra do not vary significantly, and suggest that calibrated observations of spectral line linear polarization are feasible. It is difficult to understand what in the system or processing could be causing such strong spectral variability in Stokes V and leave Stokes U in particular (formed from the same correlator products) unaffected. We also see some evidence that the Stokes Q and U spectra are shifted by 1 channel with respect to Stokes I, leading to a suspiciously Zeeman like residual when the shape of Stokes I is subtracted. This also warrants further investigation.

We recommend that spectral line linear polarization be offered for Cycle 4, but that it be stated explicitly that science cases that involve line circular polarization will not be accepted. Additionally before the call, a brief Memo should be be created and made publicly available that describes the current state of circular polarization commissioning with suitable strong wording about its lack of reliability. Additionally, a small tiger team should be formed to draw up a plan for further investigation.

1 Introduction: The Zeeman Effect

An atom or molecule with a net magnetic moment in the presence of a magnetic field will have its right and left circularly polarized emission shifted in frequency – this is called Zeeman splitting. The magnitude of the splitting is

$$\Delta\nu = g\frac{\mu_B B}{h} = ZB \tag{1}$$

where g is the Landé-g factor (and has a specific value for every transition), μ_B is the Bohr magneton of the atom or molecule, B is the magnetic field strength and h is Planck's constant. If a particular transition has a sufficiently large Landé-g factor, and the magnetic field is large enough this frequency splitting can be detectable as the Zeeman effect. In gas typical of the ISM (ignoring very strong masers, stars etc) where the splitting is small, the Zeeman effect manifests in Stokes V spectra as an S-shaped curve (rotated by 90 degrees) and is only sensitive to the line-of-sight component of the magnetic field. Conceptually this is most easy to picture in the basis with circular receiver feeds where Stokes V = RR - LL. In practice, a number of other effects can foil attempts to detect the Zeeman effect. These break down into two categories: those related to the source of emission itself and those that are instrumental. Ignoring issues related to the source for now, it has typically been assumed that all instrumental effects will manifest as "leakage" with the spectral shape of Stokes I contaminating Stokes V, such that the observed spectrum will adhere to:

$$V(\nu) = aI(\nu) + b\frac{dI(\nu)}{d\nu}. \tag{2}$$

The coefficient a is called the instrumental leakage and the coefficient $b = Z * B_{los}/2$, where Z is the Zeeman coefficient and B_{los} is the line-of-sight component of the magnetic field. Since the spectral shape of the leakage (Stokes I) is orthogonal to the expected shape of the Zeeman effect (derivative of Stokes I), the two coefficients a and b can be fit independently, and the leakage removed to reveal the true Zeeman effect spectrum. At least one hopes this is the case. In the remainder of this memo when we refer to "residual Stokes V spectrum" we mean that the fitted $a * I(\nu)$ leakage has been removed from Stokes V. Note that in standard practice the leakage is fitted and removed pixel-by-pixel (for all strong Stokes I pixels) so a residual cube can be formed accounting for the variable Stokes-I like leakage across the beam – this is the residual Stokes V cube. Some cm-wavelength results for interferometric HI and OH Zeeman can be found for example in Brogan et al. (2001a, 2001b, 2013).

Because of the dependence of the Zeeman measurement on 1/frequency it is an unfortunate fact that the Zeeman effect becomes harder to detect (all other things being equal), the higher in frequency one makes the attempt. Additionally, there are few molecules with substantial magnetic moments, and Landé-g factors. Indeed, for many complex molecules the Landé-g factors remain unknown.

2 ALMA Zeeman EOC Observations

2.1 CN (1-0)

To date, the Zeeman effect has only been reported at frequencies detectable by ALMA for the CN molecule in the (1-0) transition (113.49 GHz) and (2-1) transition (226.87 GHz) toward a handful of sources, mostly with single dishes (Crutcher et al. 1999; Falgarone et al. 2008; Crutcher et al. 2014). The CN molecule is particularly promising because of its hyperfine structure. Each of the hyperfine components has a different sensitivity to the magnetic field due to differing Landé-g factors and this can be used to provide additional constraint to the Zeeman fits.

Because of the limited availability of the necessary instrumentation, almost all of these previous detections are for sources in the North, difficult or impossible to observe with ALMA (DR21 and W3(OH) for example), or happened to be up only during the day during the EOC period for this activity (Orion). Thus it was decided to make the first ALMA attempt using the CN (1-0) transition for the massive star forming region M17-SW. A tentative single dish detection had been reported for this source by Falgarone et al. (2008) though no spectrum was shown. Because of the large single dish beam used for the reported detection we first made a small single-execution mosaic to pinpoint the exact location of the strongest CN emission in the M17-SW cloud. After that, three usable sessionized observations of the optimal single Band 3 pointing were carried out toward M17-SW:

```
April 20, 2015 1.5 exe uid___A002_X9eb5ce_X1343, X1563
May    6, 2015 2   exe uid___A002_Xa01115_X2f0, Xd6
May    8, 2015 4   exe uid___A002_Xa018c4_X11dd, X1ac2, X2017, X2537
```

After combination of all the viable data to improve the S/N, these observations did not yield any residual Stokes V signal (after accounting for Stokes-I like leakage) that seemed promising as a detection of the Zeeman effect – certainly not at the level required for a confirmation of a new ALMA mode. Indeed, while the hyperfine structure of CN makes it a great Zeeman molecule, its other features tend to inhibit Zeeman detection, like the tendency of the stronger components to be optically thick, and often to show complex velocity structure from the bulk motions in the cloud(s). At the time, these factors seemed like plausible reasons for the non-detection. These data are not discussed further in this report though at some point someone could perhaps scrutinize them again. The subsequent findings using the CH3OH maser suggest this would not be a fruitful use of time unless the issues with ALMA Stokes V are sorted and amenable to correction.

2.2 95.1 GHz CH_3OH masers

After failing with CN (1-0), it was decided to try to assess the circular polarization in a simpler kind of emission - namely 95.16944 GHz CH_3OH $8_0 - 7_1$ A^+ Class I masers. These masers have very compact emission and typically simple narrow velocity structure since they arise at shock interfaces when there is velocity coherence along our line of sight. Compact emission was an important consideration because by this point the array had moved to its most extended Cycle 2 configuration and observations of thermal gas had become impractical due to surface brightness limitations. There are three properties of these masers that should be kept in mind:

- In contrast to Class II CH_3OH, H_2O, SiO masers etc, Class I CH_3OH masers are NOT thought to be significantly time variable on timescales of several years.

- Recent private communications with Wouter Vlemmings (a methanol maser polarization expert) calls into question whether the circular polarization of Class I masers should be interpreted as due to the Zeeman effect. The question is significantly confused by the presence of multiple unresolved (in frequency space) hyperfine components (each with potentially different response to the magnetic field) that make up the line emission. However, this remains an open question of active study. Indeed, the Zeeman effect has been reported for 36 and 44 GHz CH_3OH class I masers, no Zeeman detection has been previously been reported for the 95.1 GHz transition.
- The Landé-g factors for CH_3OH transitions remain unknown (or at least unpublished). Thus, one can only presently fit for the product of $Z * B_{los}$ if one is using a Zeeman interpretation for the circular polarization.

After searching the literature, two strong southern 95.1 GHz CH_3OH maser sources (both forming massive protoclusters) close enough together on the sky to share a phase calibrator and thus be observed simultaneously were identified: G06.05 (M8E, Val'tts et al. 2000) and G10.34. One of these, G06.05 has a VLA 36 GHz CH_3OH maser Zeeman detection reported in the literature (Sarma & Momjian 2009). A test was first run on July 31, 2015 from which it became clear that the literature position for the strongest maser in G06.05 was not very accurate (missing the phase center by about $4''$) and that G10.34 (about which less was known) has two strong regions of maser emission but they are separated by about $20''$ and are 2-3 times weaker than the strongest in G06.05. G06.05 also shows a few other maser components but all within a radius of about $4''$. These data were inadvertently taken with a factor of two poorer spectral resolution than currently possible and while they showed a hint of what appeared to be Zeeman signal in the residual Stokes V spectrum (particularly in G06.05), it was clear the best spectral resolution would be needed for a solid measurement.

For the next observations on Aug. 4, 2015, the best possible spectral resolution was used and the phasecenter for G06.05 was moved to the location of the brightest maser. In these data, near the maser peak position, we see what looks like a classic and strong Zeeman signature. However, alarmingly, the residual Stokes V data from Aug. 4 have have the **opposite sign and different magnitude** to what had been observed on July 31 when it wasn't at the phasecenter. Albeit the poorer spectral resolution of the July 31 data made direct comparison difficult, this did not seem a plausible explanation for the reversal though it could explain the magnitude difference. Discussions with Bill Cotton, George Moellenbrock and others made us begin to worry about Stokes-V off-axis in general. We then decided to drop the weaker 95.1 GHz maser source (G10.34) and instead observe G06.05 at 5 different phasecenter positions. Field 0 has the brightest maser at the phasecenter, the other phasecenters ranged from 2-8$''$ from the brightest maser. Three sessions were carried out successfully for this setup. To summarize the useful observations (with highest spectral resolution):

```
Aug  4, 2015 2   exe uid___A002_Xa75b91_X57, X698
Aug 20, 2015 3   exe uid___A002_Xa88a16_X1cf, X5cb, X942
Sep 12, 2015 1.4 exe uid___A002_Xaa0bd0_X46b, X99a
```

The final spectral setup included 4 spws with the same center sky frequency (centered on the 95.1 GHz maser) but with bandwidths of 58, 117, 973, and 1875 GHz, respectively, and channel widths of 30.518, 61.035, 1953.125 and 7812.5 kHz. A notable property of G06.05 is that its declination is -24.5° and thus, it transits very close to elevation= 90° at ALMA. This means that data taken near transit is highly suspect due to degradation of the pointing model. For example, the 2nd execution of the Aug 20 session has elevation $> 80^\circ$.

In the analysis that follows, we assess the Stokes-I like leakage and the residual Stokes V signal for G06.05 for the three sessions described above. We also investigate somewhat the effect of leaving out data close to transit. **Given the caveats stated above regarding the interpretation of polarization measurements toward methanol Class I masers we want to emphasize that at minimum what we are looking for in these data are:**

1. **Consistency of the polarization signal across observing dates**
2. **Consistency of the polarization signal with different observed phasecenters once the polarized beam pattern is (roughly) taken into account.**

the detection of the Zeeman effect itself is a secondary goal.

3 Data Processing and Analysis

3.1 Polarization Calibration

The overall approach was to find a procedure that would most easily allow the use of the current Early Science script generator in combination with the necessary extra polarization calibration using

the polarization calibrator data. In the following description the polarization calibrator is called the POLCAL.

- Run the script generator for each execution following standard practice. The only exception is that the first execution must be completely processed before the other ones to derive the absolute flux calibration of the phase calibrator. This phase calibrator flux was then hard-coded in subsequent executions at the setjy step, and used to derive absolute flux calibration for the other targets. This is slightly painful because the executions without a FLUXCAL target are generated as if there were none, i.e. no setjy step is inserted and the gaincal steps do not include the fluxscale steps. It would be very helpful if there were a mode of the script generator that stubs in the required flux calibration based on the phase calibrator.
- Additionally, for narrow bandwidth observations, the bandpass calibrator needs to be smoothed in the bandpass steps. For reasons beyond my comprehension, the script generator has been changed to preclude this (though smoothing is always used in the pipeline for narrow spws) – so bandpass smoothing also had to be inserted manually in the bandpass step for the solint parameter.
- Once the scripts for all executions are done, for each execution the bandpass table is applied to the POLCAL. Then for each execution the bandpass-corrected POLCAL target is split off from the parent dataset and the results are concatenated.
- All other targets have their full suite of normal calibration applied and the corrected column is split off. These "standard calibration applied" datasets are then concatenated.
- From this point the processing of the bandpass-calibrated POLCAL data follows a similar path to that of the 3C286 casaguide. A sample script for the Aug. 20 session is appended to the report. One should pay careful attention to:
  1. A plot of the first gaincal solve for phase vs time caltable with poln='/' should show a smoothly varying trend with parallactic angle change as a function of time.
  2. A plot of the first gaincal solve for phase vs time caltable with poln='/' should show very small values for XX/YY solutions for the reference antenna. Note that the plot often prints a very small multiplicative number at the top left of the plot, of 10^{-6} for example, that if unnoticed can make it seem like the XX/YY difference is very large rather than very small. If a large difference is seen this is an indication that the current reference antenna is unsuitable – this will happen if the reference antenna switches at all during the first gaincal solve due to inadequate signal-to-noise on the POLCAL, time-specific flagging of the POLCAL etc. This is very important – a poor choice of reference antenna here can completely foil the polarization calibration downstream. The normal machinery to keep things lined up when a change of the reference antenna is induced cannot work correctly for the absolute XX/YY phase ratio because the zero-point is unconstrained.
  3. It is essential that qufromgain correctly decodes the feed offset position. Cycle 3 changes to the spw names foiled this for a while but has been fixed in the CASA 4.5 release.
  4. The polarization model derived in the first run of qufromgain on the first gaincal table should be consistent across spws. If not its a sign that the POLCAL is insufficiently polarized and/or the S/N is too low in general. One can try some time averaging rather than solint='int' in the preceding gaincal solve, but one should not time-average over significant changes in parallactic angle. Empirically it seems that a total polarized intensity of $> 1.5\%$ is required for good results, at least in the presence of some narrow spws.
  5. The Q and U derived during the XYf+QU stage should be consistent across spws, if not, time pre-averaging and spectral smoothing can be applied. It is important that the feed-offset positions in the data are correct for this solve. There are currently issues for PM02, PM03, and all the CM antennas in the TMCDB (ICT-1821).
  6. If spectral smoothing is required for good results in the XYf+QU solve, it should also be used for the polcal solve step. **it is notable that for these maser data reductions the spectral smoothing used was 7.8125MHz – 1/8 the narrowest bandwidth, and significantly wider than the maser line.**
  7. The second gaincal with the model for the POLCAL, and Kcrs, and XY0 applied on-the-fly should show a small residual polarization for the POLCAL that is noise-like for all spws. The change of XX/YY amplitude with time should be removed. An example of the comparison between the first and second gaincal amplitude of XX/YY as a function of time is shown in Figure 1.
- The resulting *.Kcrs, *.XY0, and *.Df.gen are applied to the concatenated "standard calibration applied" multi-source dataset. Then the science target(s) are split off.

The polarization calibrator used for all three methanol maser sessions is J175132+093858 and the resulting Stokes polarization vectors (I, Q, U, V] derived from the xyamb recipe are given below followed by the derived absolute flux in Jy:

```
Aug  4: Stokes vector: [1.0, 0.025828911922872066, -0.0001085052617781912, 0.0] 5.4
Aug 20: Stokes vector: [1.0, 0.068612365052103996, -0.0044264671159908175, 0.0] 7.2
Sep 12: Stokes vector: [1.0, 0.043925805948674679,  0.022970088757574558,  0.0] 5.3
```

This comparison demonstrates a surprising amount of variability in the polarization properties of this POLCAL. These changes are not obviously correlated with changing flux, however, the absolute flux densities are currently fairly uncertain due to poor FLUXCALs being employed for some of the sessions (Pallas on Aug. 20). Regardless these results mean that polarization monitoring of POLCAL targets is essential to ensure that the polarized intensity remains strong enough for successful polarization calibration, as the strength of the POLCAL itself cannot be used as an indicator.

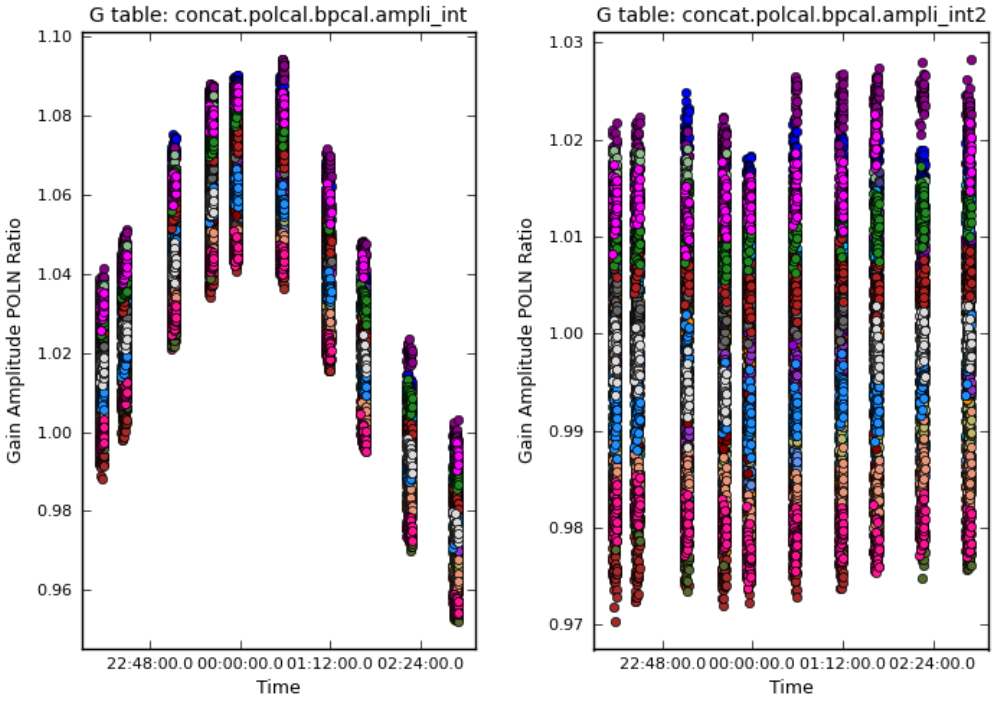

Figure 1: Comparison between the first and second POLCAL gaincal steps of XX/YY amplitude for the Aug. 20 session. The first (left) showing the expected initial variations with parallactic angle and time and the second (right) showing a ratio near one when a correct Stokes Vector is used for the solve. Note the difference in scales.

3.2 Polarization of Science Target

After applying the standard calibration and the polarization calibration the science target data were split off. The continuum emission was subtracted and the strongest maser channel was used to self-calibrated the line data. At each of these stages it was first checked that the processing did not affect the shape of Stokes-V. Indeed, while the self-calibration made a large improvement to the appearance of Stokes I due to the initial dynamic range limitations, it made almost no difference to the ratio of Stokes-I to Q, U, or V, as all the Stokes parameters increased in magnitude by similar amounts. The phasecenter of all the images was explicitly defined in clean to be the same position (near the peak of the brightest maser), regardless of the observed phasecenters so that all images share the same pixel values.

In what follows, we assume that Stokes V can be characterized by Equation (1) whether or not the fitted coefficient on the derivative can be interpreted as proportional to the magnetic field (i.e. Zeeman effect). We used two methods to evaluate the spectra. First Todd wrote a method in python/CASA to fit for coefficients a and b in Eq. 2 for a given pixel using an input Stokes I and V cube – this method (tt.zeeman) creates spectral plots for the specified pixel that can be used to assess the fit. It uses 1000 Monte Carlo simulations to derive error estimates on the fits for the a and b coefficients. This method is not yet in analysisUtils but could be ported there if requested. Second, the tried and true 'Zeemap' task in Miriad was used to fit and solve for a and b at every pixel in the cubes above a Stokes I threshold of 4 Jy/beam. This method also produces error estimates, and the resulting maps of the $2 * b * \Delta\nu$ were subsequently masked where the $S/N < 3$. These two methods show excellent agreement in both value and error estimates. If at some point in the future it seems worthwhile, Todd is willing to expand his python/CASA method to create maps to replace the use of Miriad.

4 Stokes V Leakage pattern

Figure 2 shows the Stokes V beam map in azimuth/elevation coordinates for Band 3 from C. Hull's report, which reflects the Band 3 feed angle of -10° offset from the vertical plane (Carter et al. 2007). This pattern is what one would see when observing at parallactic angle of 0°, and will be rotated on the sky for observations from different parallactic angles. When data from many parallactic angles are included in a single image the superposition of all the parallactic angle-specific Stokes V beam maps manifests as the "leakage map". In order to demonstrate that our datasets detect this beam pattern, we examine the data from the individual executions which were obtained over a small range of parallactic angle. Because the target G06.05 transits close to the zenith, the parallactic angle rotates rapidly through nearly 180°. Thus, the data obtained up to an hour before and after an hour after transit show only a small change in parallactic angle (see Figure 3), and correspond to -90° and +90° rotations of the leakage pattern. The corresponding leakage maps obtained on August 20, 2015 (Figure 4) demonstrate that the leakage observed toward the brightest maser (the northern peak) is: (1) of opposite sign when observing field 3 vs. field 4, and (2) reverses sign when the sky has rotated from -90° to +90° parallactic angle. These two results are consistent with the leakage pattern, because fields 3 and 4 are offset in declination from field 0, meaning that the bipolar axis of Figure 2 is aligned nearly along the north/south direction. Also, the magnitude of the leakage is larger when observing field 4 compared to field 3, consistent with the fact that field 4 is about twice as distant from field 0. A consistent result is seen in the September 12 dataset (Figure 7) for which both executions were observed post transit, giving confidence in the time stability of the Stokes V beam map.

5 Residual Stokes V

5.1 No Consistency for the Same Phasecenter, Different Days

No consistency for the Residual Stokes V is seen across different days for the same phasecenter. Figure 8 shows the fitted b coefficient for Field 0 (bright maser at the phasecenter) for Aug 4, Aug 20, and Sept 12. As you can see there is no correspondence between the derived coefficient. Indeed, one of the most disconcerting things about this analysis is the apparently very good fit for pixel 218, 221 on Aug 4 that is very suggesting of a Zeeman detection, that is completely absent from the other two days. Figure 9.

5.2 No Consistency Within the same Day across Different Executions or Different Phasecenters

Perhaps the lack of consistency in the residual Stokes V between days for the same phase center could be attributed to some sort of polarization time variability in these 95.1 GHz masers? We also explored how the residual Stokes V varies as a function of phasecenter on Aug. 20 and Sept. 12. Here we focus on Aug. 20 since it has much higher sensitivity. First in Figure 10 we show the fitted b coefficient from each of the three Aug 20 executions evaluated independently, with each of the five phasecenters shown. Little correspondence is seen across phasecenters or across executions. Most disturbing is the lack of agreement across executions for Field 0 – this has the bright maser at the phasecenter and thus should be subject to the least amount of primary beam effects. Next we show the combined Aug. 20 b coefficient across fields, again there is little correspondence across the different phasecenters: Figure 11 shows the maps while Figure 12 shows the spectra from a position near the peak of the bright maser.

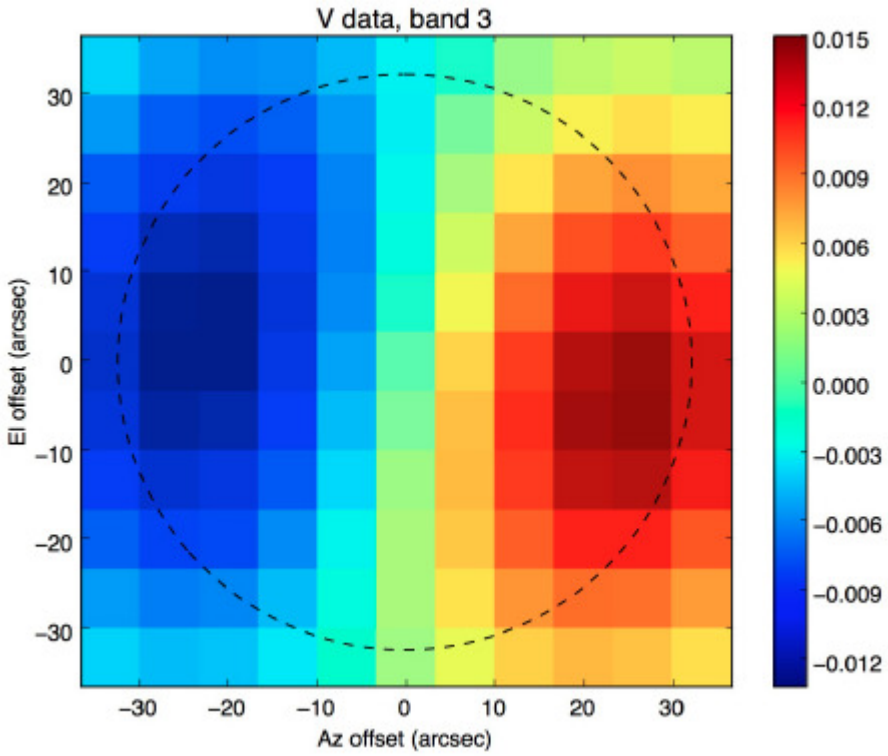

Figure 2: Reproduction of the Stokes V beam map from Figure 2 of C. Hull's polarization beam mapping report. The circle shows the FWHM of the beam. The bipolar pattern is aligned at an angle, consistent with the -10° offset of the Band 3 feeds from the vertical plane of the cryostat.

6 Linear Polarization

So far we've found that the Stokes V "Leakage" appears consistent with expectations for the behavior of the Stokes V instrumental beam pattern. However, we've also found a very disturbing complete lack of **spectral** consistency between residual Stokes V measured (1) on different days, same phasecenter; (2) same day, different phasecenters; (3) same day, different executions, same phasecenter; and (4) different executions, same day, different phasecenters. One possibility is that there is a significant, time variable spectral instrumental polarization signal that is not being calibrated by the polarization calibration procedure. Such a signal could affect just the cross hand correlation products or all four correlation products. One way to explore this is to look at the linear polarization properties of the masers. Recall that for linear feeds Stokes Q = XX - YY, but like Stokes V, U is composed of only the XY and YX cross hands. Thus, one might expect to see spectral oddities in Stokes U that are not evident in Stokes Q if the residual spectral instrumental signal is limited to the cross-hands. We do not see this.

To illustrate the properties of the linear polarization signal and take advantage of existing software we have fit the Stokes Q and U spectra in the same way as described for Stokes V. This does not have any particular meaning physically but serves to examine what Q and U look like spectrally after removing a component that is proportional to Stokes I (i.e. the a coefficient). For example, if the Q and U look spectrally exactly like Stokes I, after removing $a * I$ the residual will be noise like. Figure 13 shows the results of this analysis across the three observing sessions, while Figures 14 and 15 show the same pixel but for the five phasecenter positions from Aug. 20. What we find for Stokes Q and U are that

- Both Q and U show significant spectral deviations from the shape of Stokes I
- Q and U have very similar spectral shapes (though they can be of opposite sign)
- The spectral shapes of Q and U do not vary significantly with observing date for the same phasecenter
- The spectral shapes of Q and U do not vary significantly with phasecenter on the same observing date

As a final statement on the linear polarization results, while the stability of the signal in Q and U is gratifying, we have no idea what the physical meaning is of their $dI/d\nu$-like residual shape – it

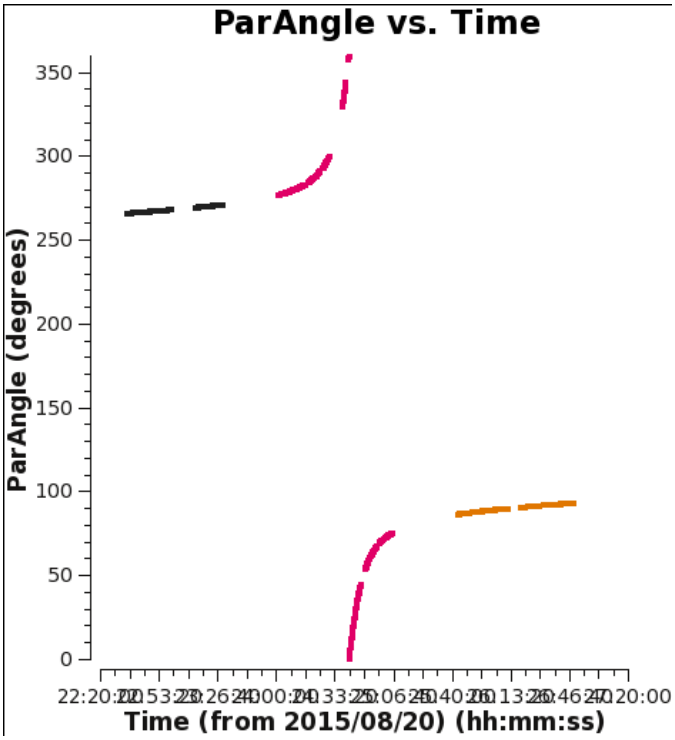

Figure 3: The parallactic angle coverage of the methanol maser target colorized by observation ID of the August 20, 2015 dataset. Note that during ObsID 0 it is essentially constant at -90°, while ObsID 2 it is essentially constant at +90°.

definitely shouldn't be taken as some manifestation of the Zeeman effect. It would be remarkable but not impossible if these are the true linear polarization shapes of the masers are – i.e. possibly due to differing responses of the various underlying hyperfine components to the magnetic field. Overall, it looks suspeciously like there could be a 1 channel shift in Q and U with respect to Stokes-I. This should be further investigated in the future.

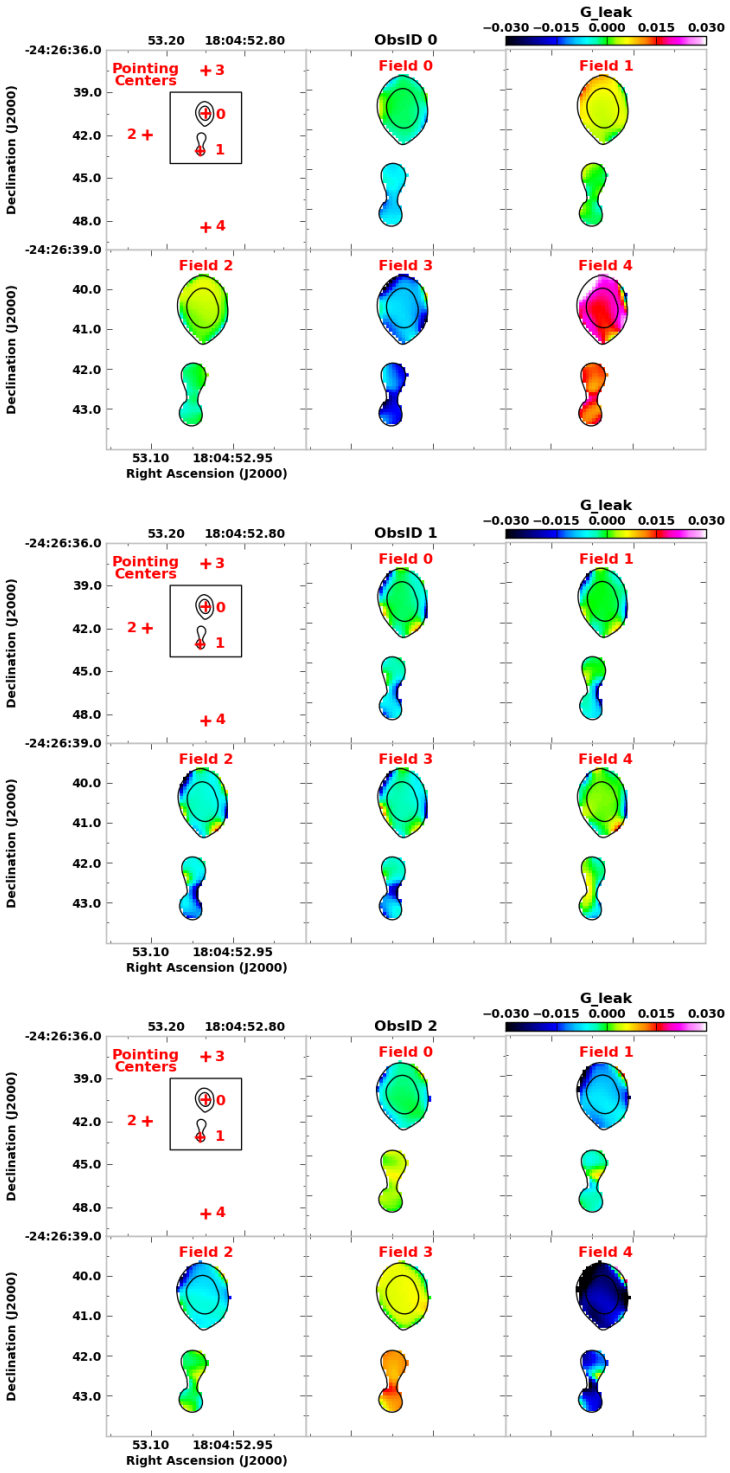

Figure 4: The fitted Stokes-I like leakage from Aug. 20 observed for each of the 5 mosaic pointings, with each of the three executions assessed independently. The colorscales are the same for all three sets of plots. The first panel in each plot shows the locations of the 5 phasecenters, and contours from the Stokes I peak moment image at 4 and 40 Jy/beam. The other five panels show the data from each phasecenter zoomed in to the box shown in the first panel. Top plots: ObsID 0 in which parallactic angle was nearly constant at -90°; Middle plots: ObsID 1 in which parallactic angle ranged from -80° to +80°; Bottom plots: ObsID 2 in which parallactic angle was nearly constant at +90°. The plots are consistent with the expected behavior of the Stokes I like leakage.

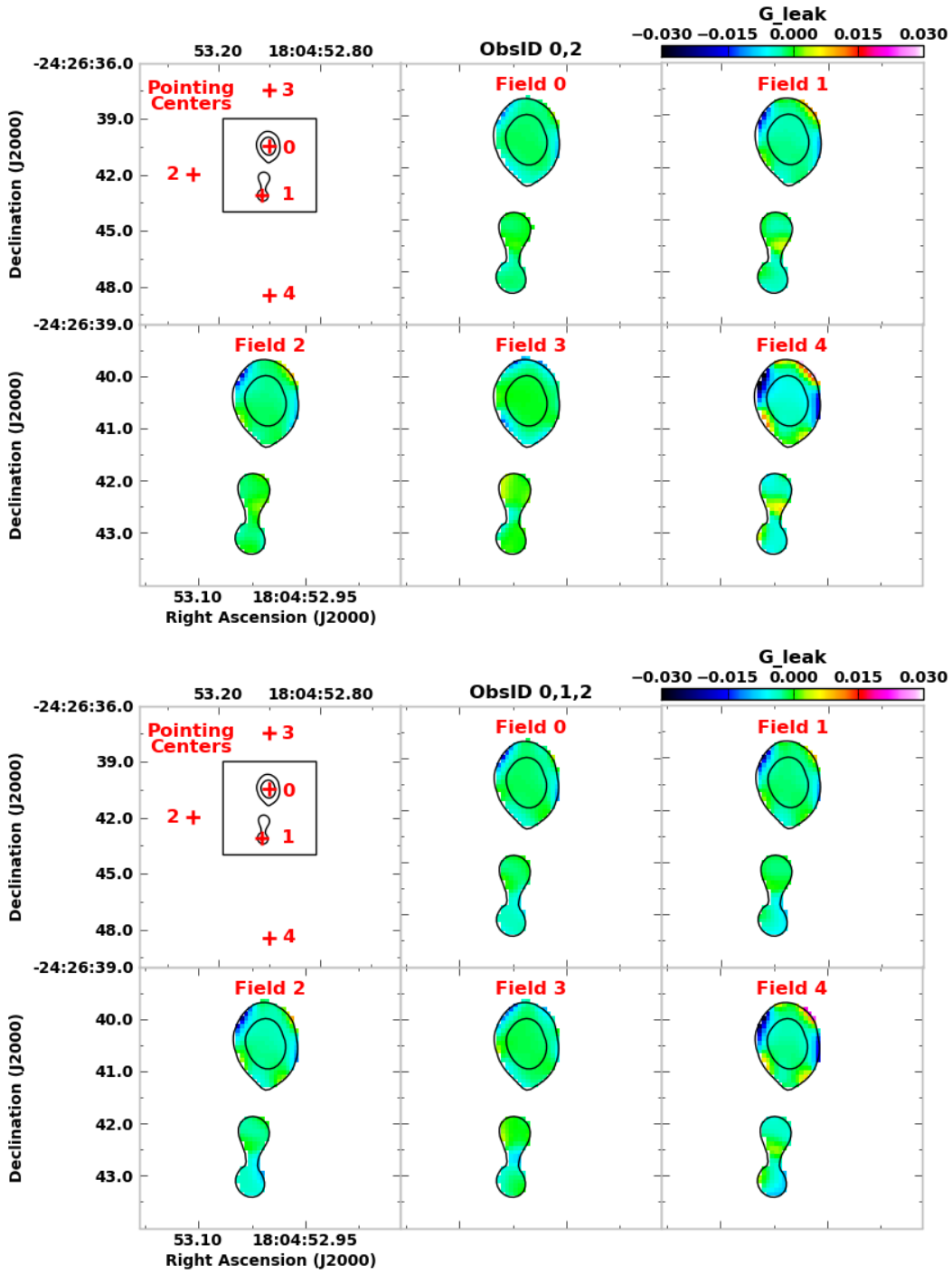

Figure 5: The leakage observed for each of the 5 mosaic pointings using data from combined ObsIDs. Top panel) ObsIDs 0 & 2; Bottom panel) ObsIDs 0,1,2. For comparison these are shown on the same scale as Figure4 and show that when data are combined over a range of parallactic angle, much of the leakage averages out.

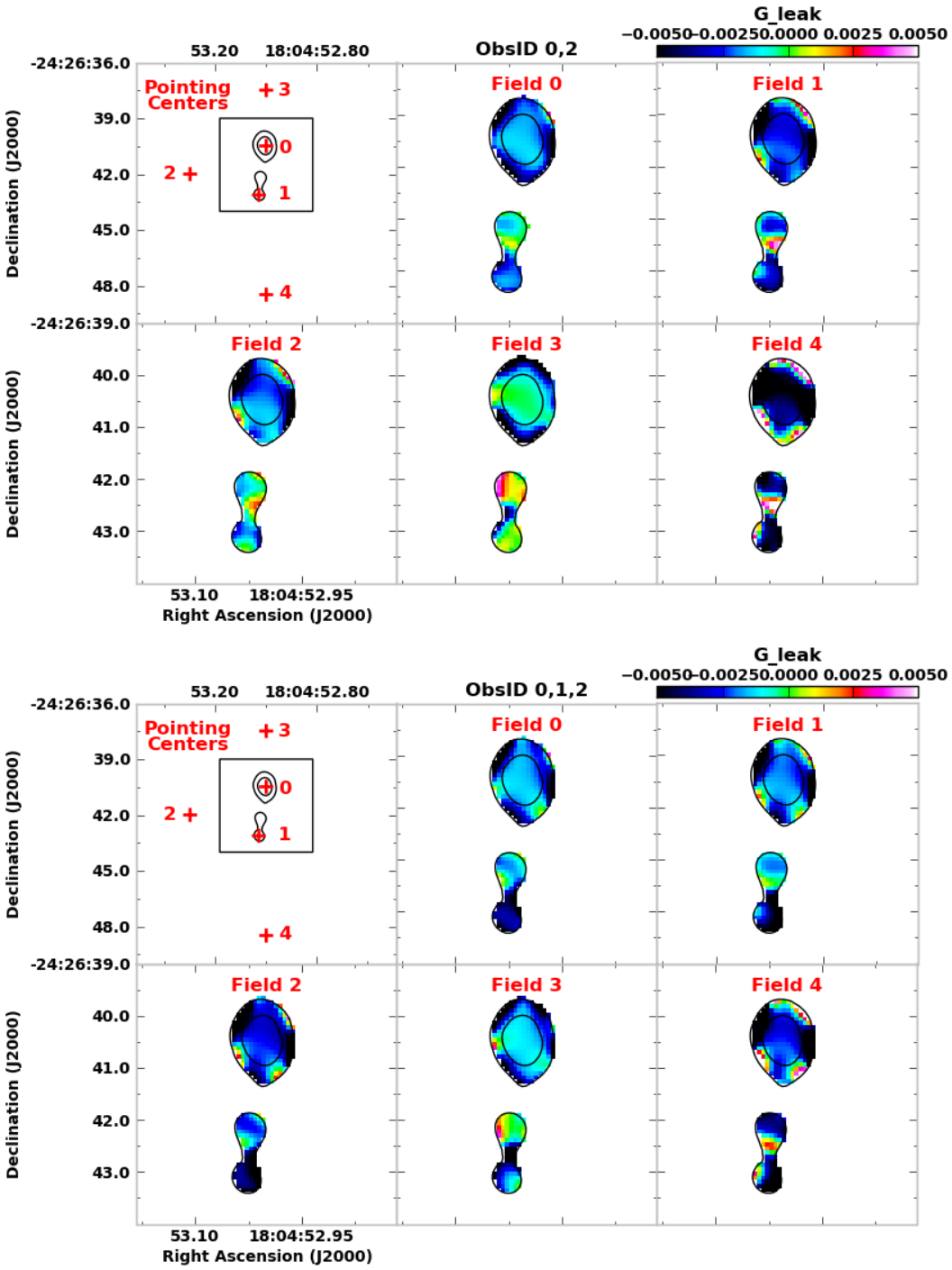

Figure 6: Same as Figure 5 for the combined datasets (top ObsIDs 0 & 2, bottom ObsIDs 0, 1, 2), but the colorscale for the images have been stretched to show the detail at small values of the leakage.

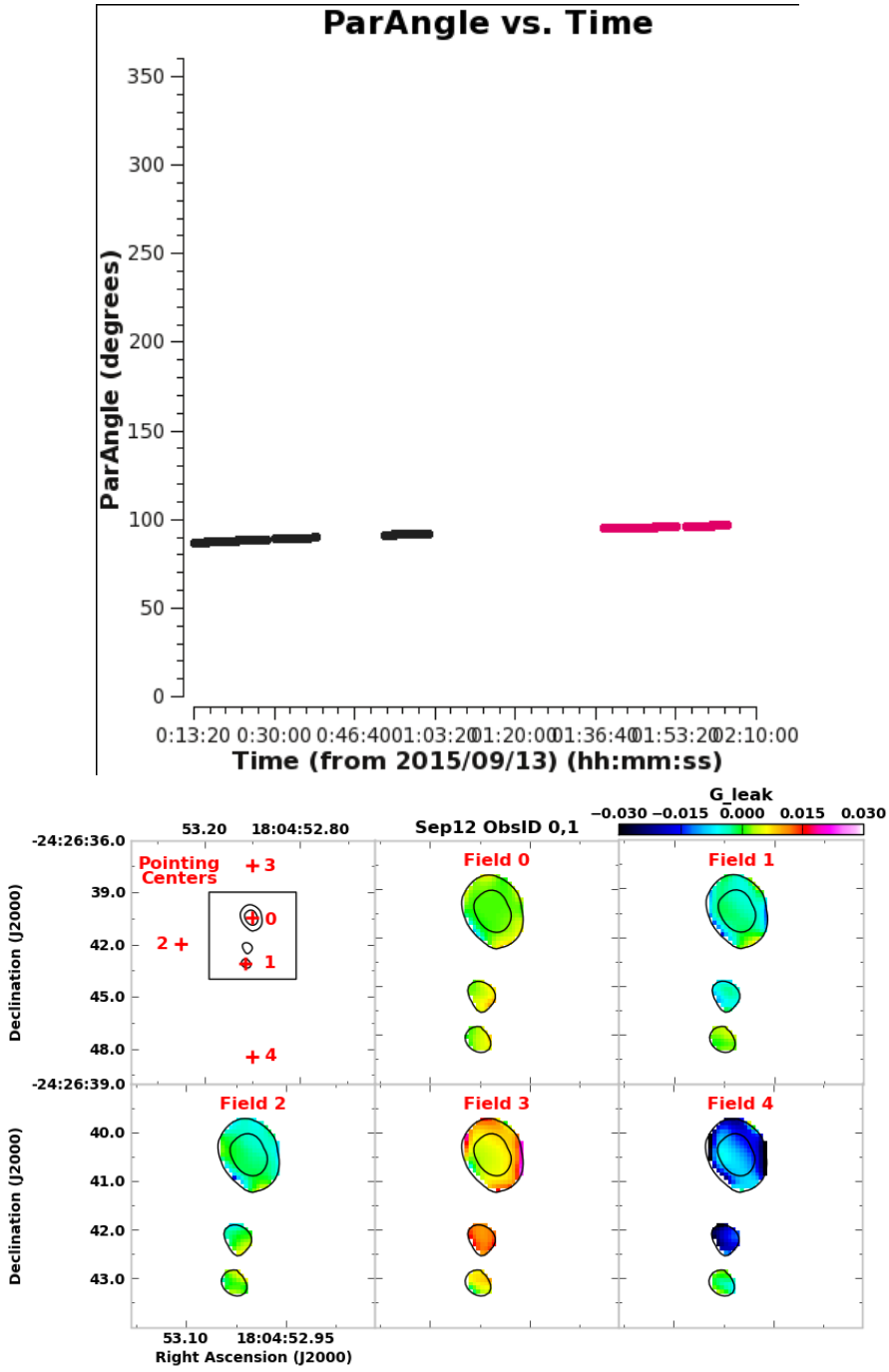

Figure 7: Top: The parallactic angle coverage of the two executions on Sept 12, 2015, both of which were post-transit; Bottom) the leakage observed for each of the 5 mosaic pointings using data from combined ObsIDs, which is similar to the result for ObsID 2 of Aug 20.

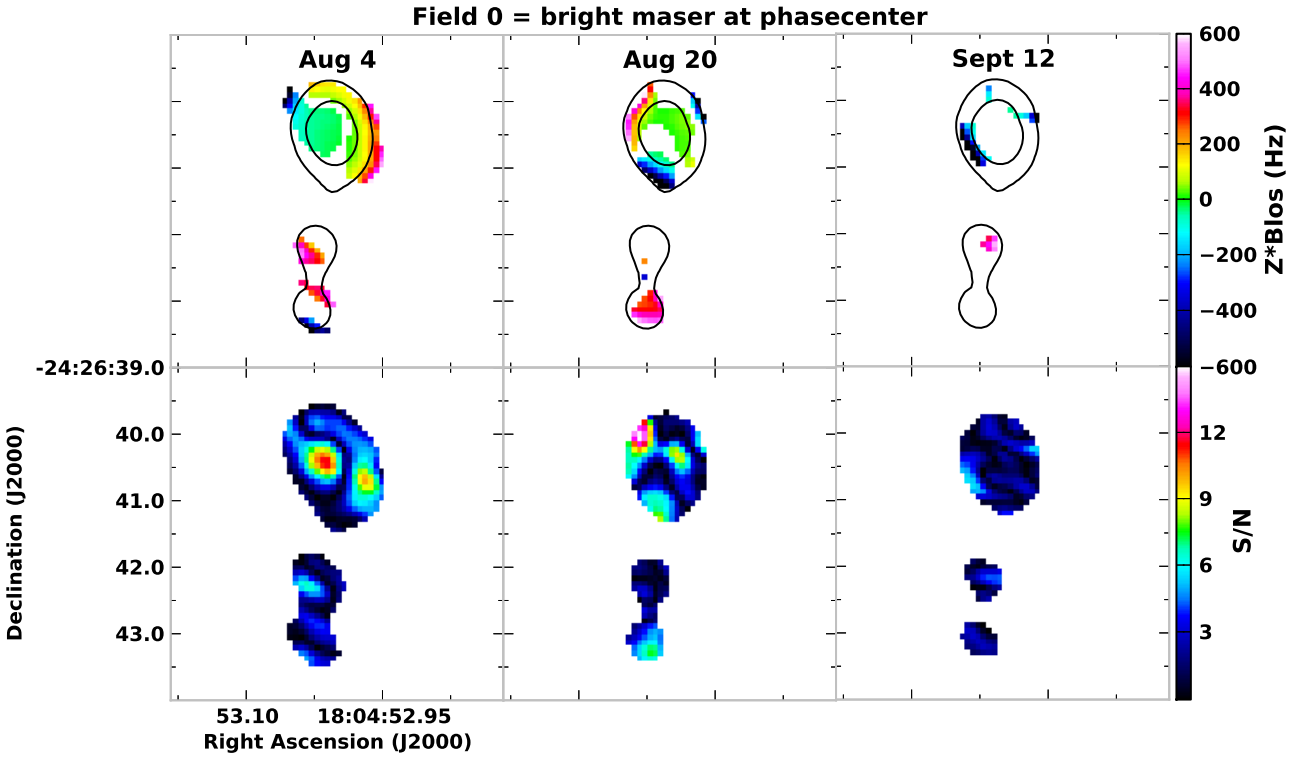

Figure 8: Top: Fitted b coefficient for Field 0 (brightest maser at the phasecenter) for the three different sessions on Aug 4, Aug 20, and Sept 12. Bottom: The S/N ratio of the fits – the top panels have been masked for $S/N < 3$. The 4 and 40 Jy/beam Stokes I contours from Aug. 20 are overlaid for reference.

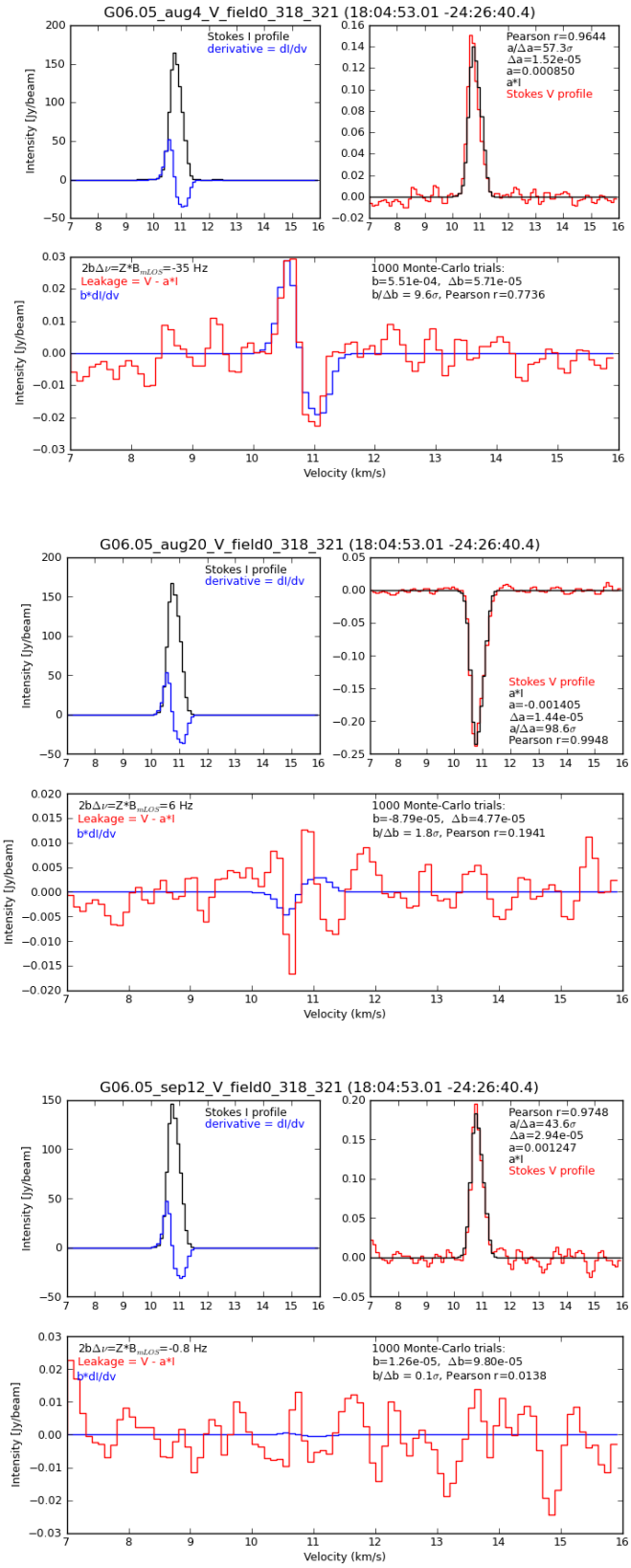

Figure 9: Spectral plots for pixel 218, 221 near the bright maser peak for Field 0 for each of the three sessions showing disagreement in the spectral shape of the residual Stokes V and hence the fitted b coefficient (this pixel has the highest S/N b fit from Fig.8 for Aug. 4). Though noisier, the Sept 12 data should have shown the residual Stokes V signal apparent on Aug 4 if it were present and Aug 20 shows a completely different shape.

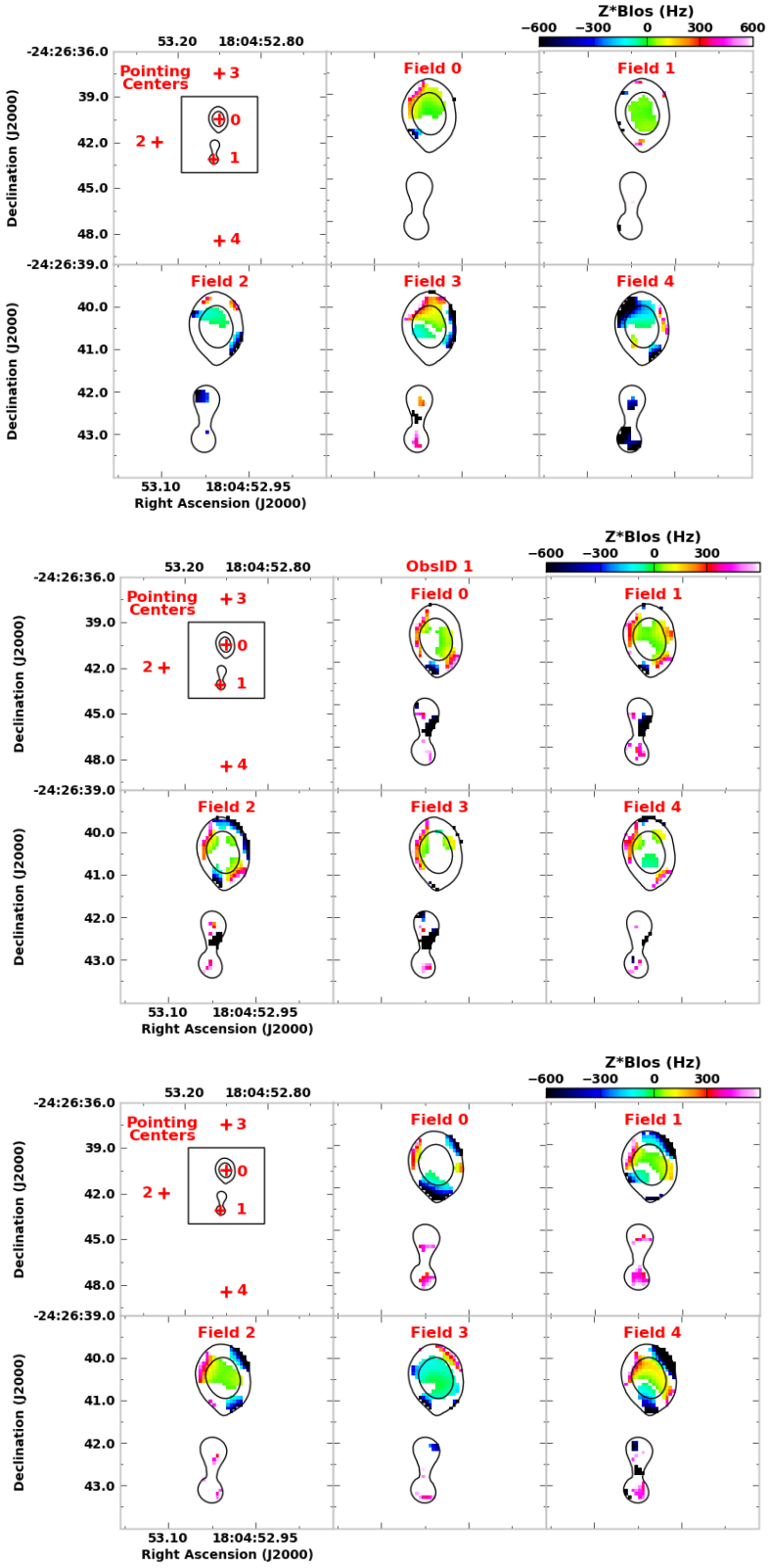

Figure 10: Maps of the Aug 20 fitted b for each phasecenter masked at fitted $S/N < 3$. Top: First execution; Middle: Second execution; Bottom: Third Execution. Recall that the middle execution was taken very near elevation=90° but this seems to have little impact on the outcome as the first and third executions also show little correspondence.

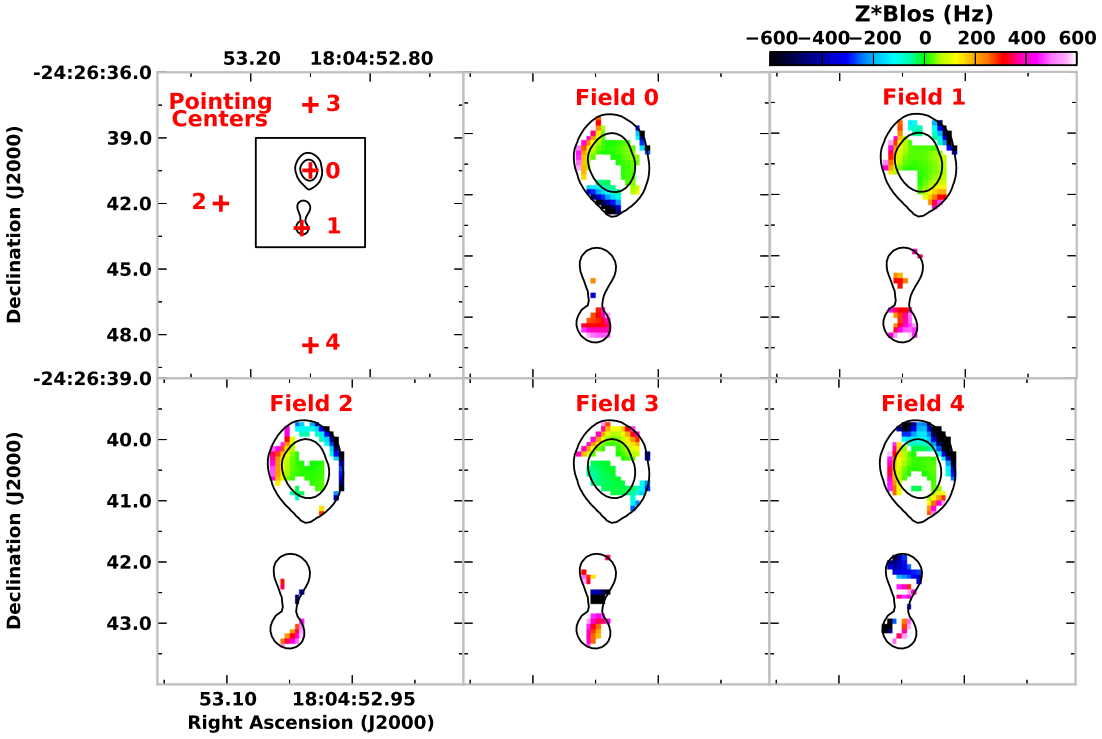

Figure 11: Maps of the fitted b for each phasecenter for Aug 20 data combined, masked at fitted $S/N < 3$.

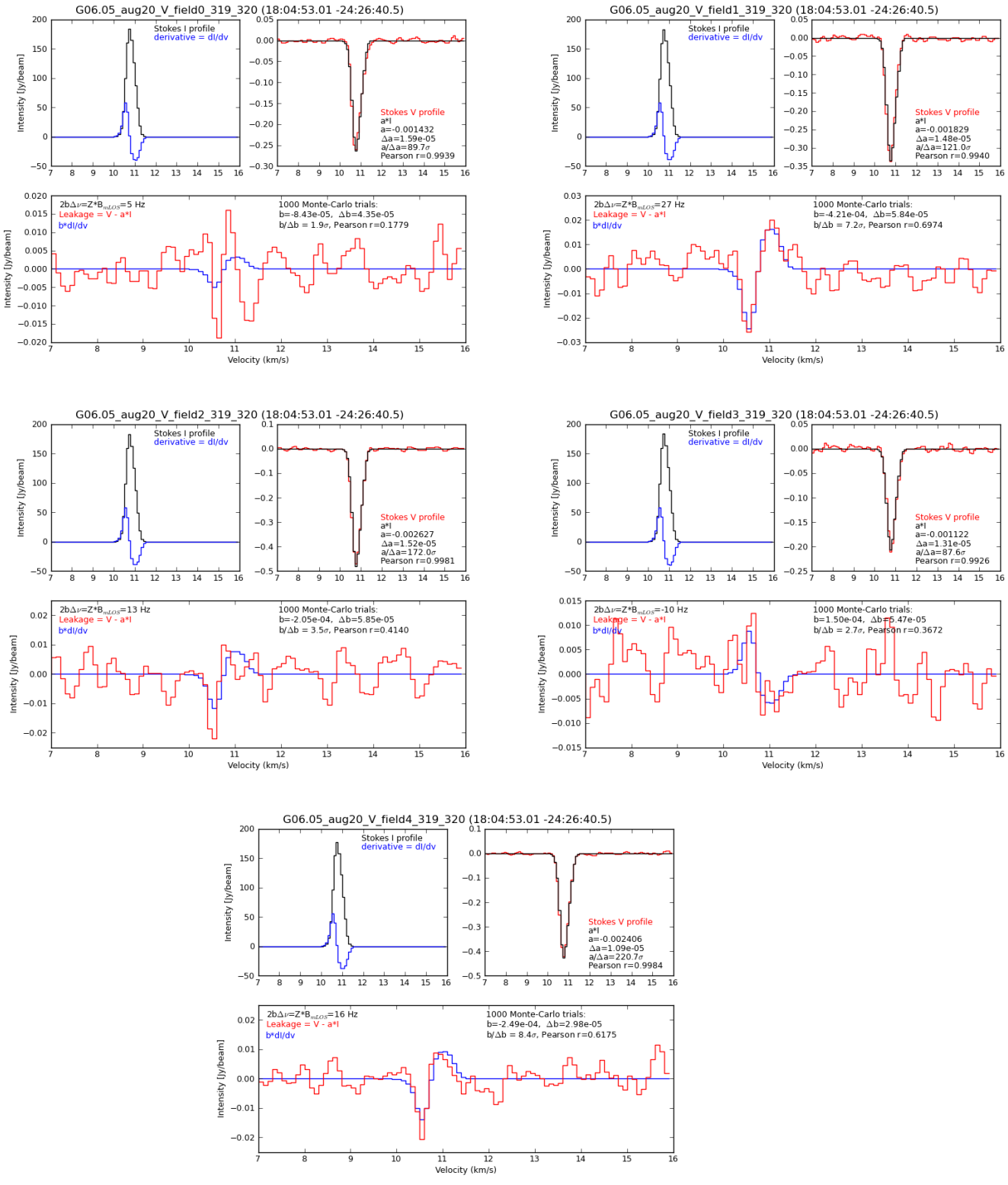

Figure 12: Spectral plots of Stokes V (Red) for the five phasecenters observed for Aug. 20 for the same pixel (319,320) near the maser peak. The locations of the phasecenters (Fls -ields 0..4) with respect to the bright maser are shown on Figure 11. Note that the residual Stokes V spectra (Red curve in bottom panel of each plot) shows little correspondence from phasecenter to phasecenter – between fields 1 and 3 it even changes sign. Additionally for Field 0, which had the bright maser at the observed phasecenter there is no detection of an S-like Zeeman pattern.

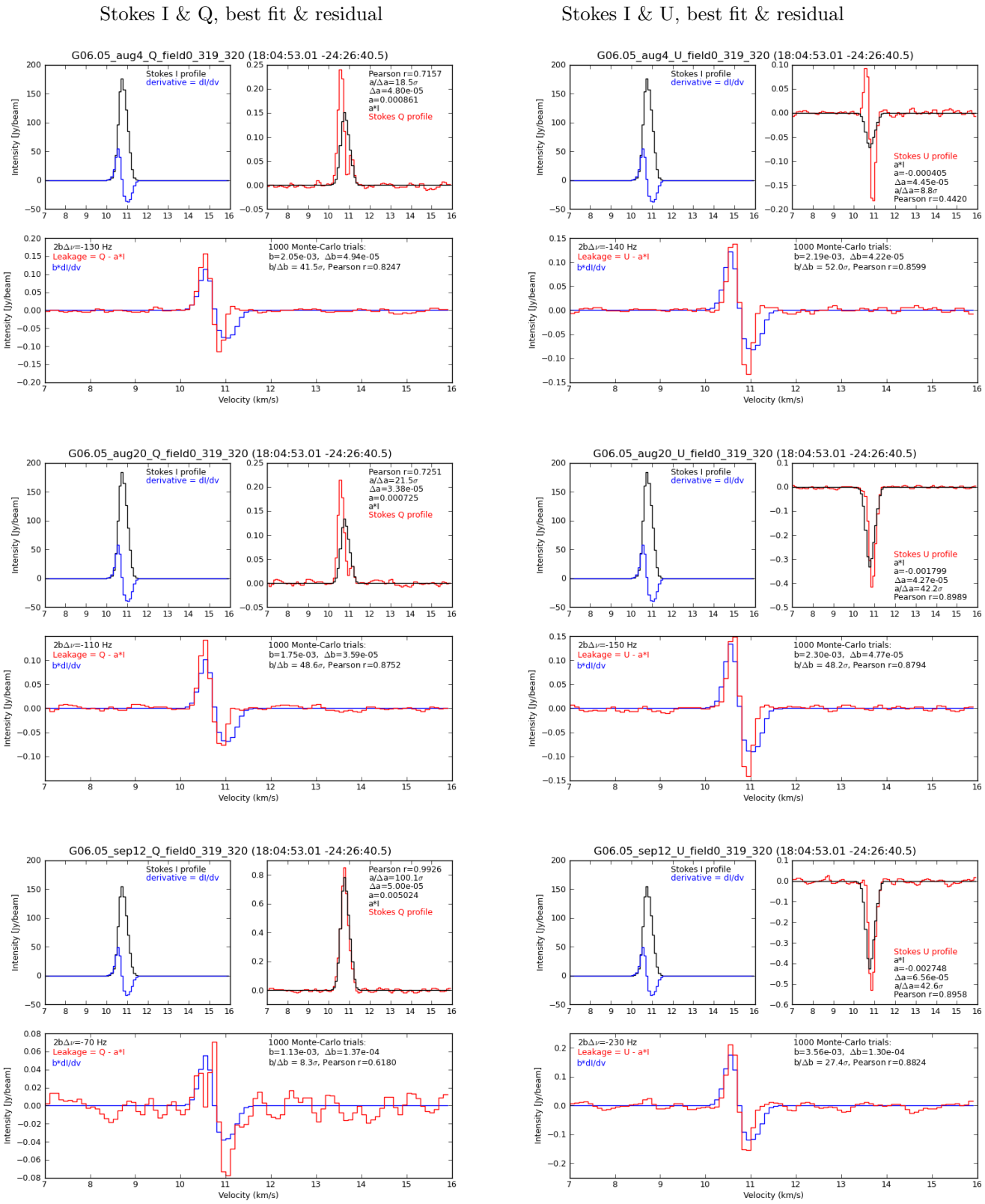

Figure 13: Left column: Stokes Q and its residual after removing a Stokes-I-like fit. Right column: Same for Stokes U. The rows are the three different days of observation. The residual Stokes Q and U are pretty consistent in shape across the three sessions. However, note that the y-axis scale in the residual intensity plots is factors of 5-10 larger in Q and U than in the Stokes V plots in Figure 9 and Figure 12. These Stokes Q and U residuals should not be taken as the Zeeman effect.

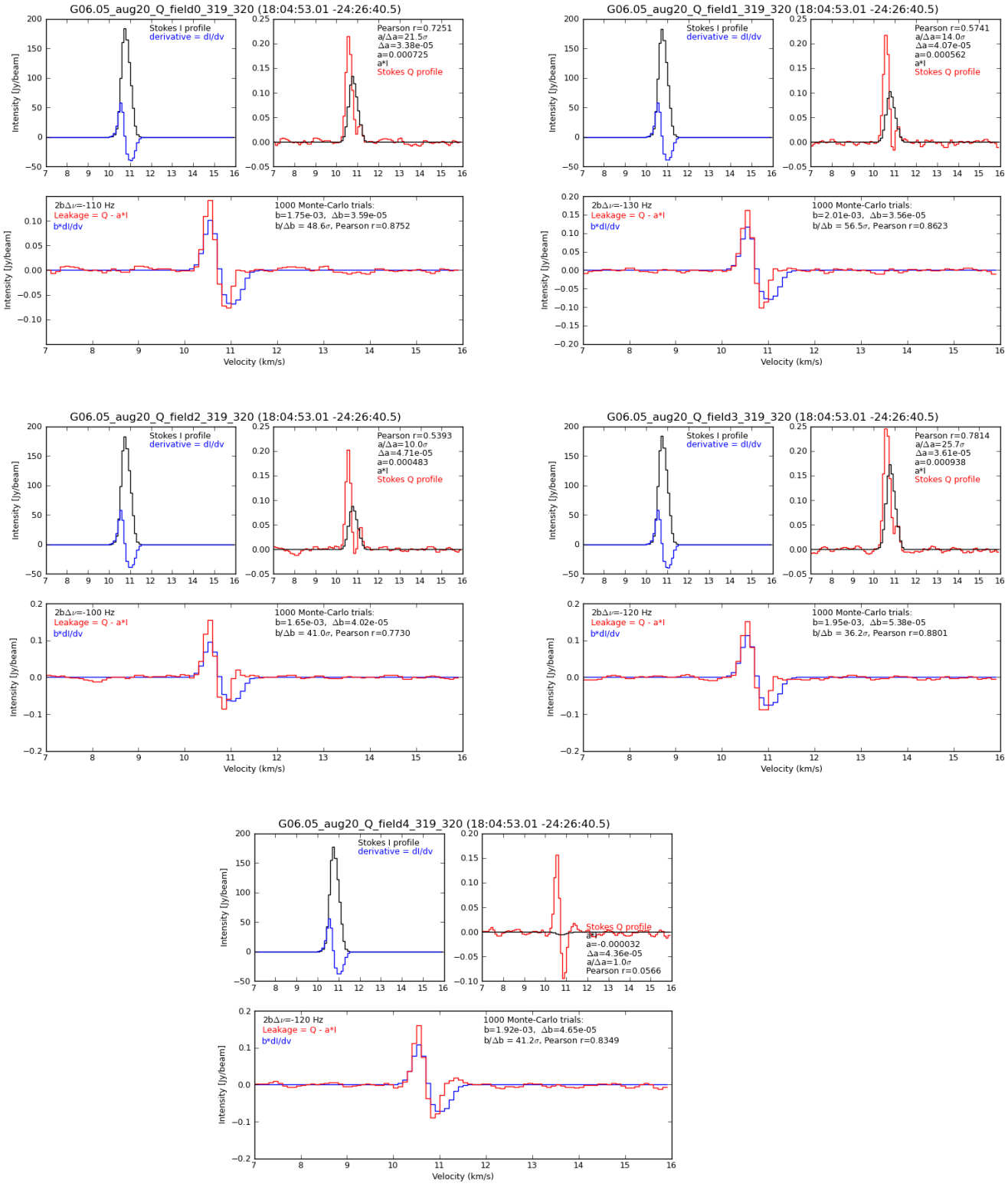

Figure 14: Spectral plots of Stokes Q (Red) for the five phasecenters observed for Aug. 20 for the same pixel shown in Figure 13 and Figure 12. These Stokes Q residuals should not be taken as the Zeeman effect.

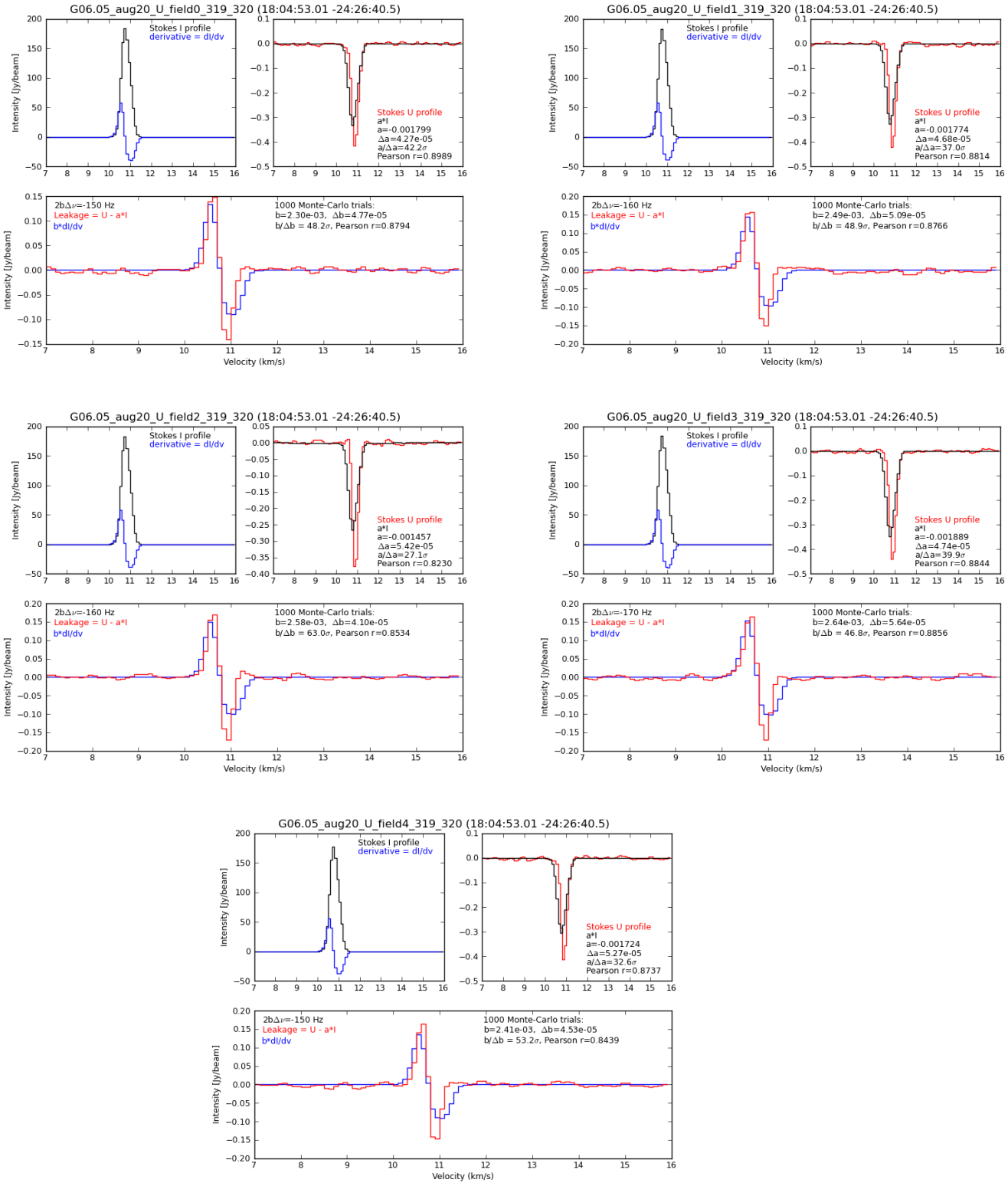

Figure 15: Spectral plots of Stokes U (Red) for the five phasecenters observed for Aug. 20 for the same pixel shown in Figure 13 and Figure 12. These Stokes U residuals should not be taken as the Zeeman effect.

References

[1] Carter et al. 2007, ALMA Front-end Optics Design Report, FEND-40.02.00.00-035-B-REP, Figure 5, http://edm.alma.cl/forums/alma/dispatch.cgi/revsactive/showFile/101736/d20070413130247/Yes/FEND-40.02.00.00-035-B-REPcomments-1-FP+NT-20070320.pdf

[2] Brogan, C. L., Goss, W. M., Hunter, T. R., et al. 2013, ApJ, 771, 91

[3] Brogan, C. L., & Troland, T. H. 2001a, ApJ, 550, 799

[4] Brogan, C. L., & Troland, T. H. 2001b, ApJ, 560, 821

[5] Crutcher presentation on unpublished work: http://adsabs.harvard.edu/abs/2014isms.confETF15C

[6] Crutcher, R. M., Troland, T. H., Lazareff, B., Paubert, G., & Kazès, I. 1999, ApJL, 514, L121

[7] Falgarone et al. 2008, A&A, 487, 247

[8] Sarma & Momjian 2009, ApJ, 705, L176

[9] Val'tts et al. 2000, MNRAS, 317, 315

[10] Wiesemeyer, H., Thum, C., & Walmsley, C. M. 2004, A&A, 428, 479